Nonlinear friction in the periodic stick-slip motion of coupled oscillators

Y. Braiman, F. Family, and H. G. E. Hentschel
Department of Physics, Emory University, Atlanta, Georgia 30322
(Received 23 January 1996; revised manuscript received 16 July 1996)

We suggest that coupling-induced orbit hopping is one possible mechanism for stick-slip dynamics. This mechanism is dominant in the highly nonlinear regime. Our example is a one-dimensional array of nonlinearly coupled oscillators subject to a strong periodic potential. The nonlinear dynamics leads to a fundamentally different friction law, in particular when the driving force is barely larger than the minimal force needed to start motion. We find a dramatic increase in the friction coefficient of the array compared to that of a single uncoupled oscillator, even though the same constant force f is applied to each oscillator in the array. The sliding friction coefficient η is found to diverge as $\eta \propto (\kappa-\kappa_c)^{-1/2}$, where κ_c is the critical value of the coupling constant κ. The coefficient η also grows linearly with the number of elements in the array N and shows dynamical transitions as the external force f applied to each of the oscillators is increased. [S0163-1829(97)07107-5]

I. INTRODUCTION

Friction between materials is of fundamental importance for many applications in pure and applied sciences.[1,2] Understanding the basic mechanisms occurring at the interface of two materials brought into close contact is significant for a wide range of technological applications, from adhesion to wear and lubrication.

The limit of small velocities leads to a special type of dynamics called stick-slip motion, which is of particular interest for many applications including friction, lubrication of materials,[1,2] earthquake models, and avalanches.[3] Recent experiments,[4] as well as theoretical models,[5] and studies of spring-block systems[6] indicate that stick-slip motion arises mainly in situations in which the average velocity of the system is low. The transition from creep motion to stick-slip[4] and sliding motion[7] is of interest, especially in small systems such as nanostructures, in motion involving boundary lubrication, and in other related phenomena. The dynamical mechanisms leading to stick-slip motion are not yet clear and studies of these mechanisms are important in understanding the basic principles of friction at a wide range of length scales from atomic[8] to macroscopic.[3]

In this work we concentrate on a possible mechanism for friction where the adsorbate-substrate interaction is strong and consider the contribution of the nonlinearity to stick-slip motion. We study a class of nonlinear systems: a one-dimensional (1D) chain of nearest-neighbor coupled oscillators, all subject to a strong nonlinear periodic potential and all driven by the same external force.

In the studies of friction one possible starting point is the equation of motion

$$m\ddot{x}_j+\gamma\dot{x}_J=-\frac{\partial U}{\partial x_j}-\frac{\partial V}{\partial x_j}+f_j+\xi_j\,, \tag{1}$$

where x_j is the coordinate of the jth oscillator, m is the mass, γ is the linear friction coefficient, f_J is the external force, and ξ_j is the noise. The oscillators are subjected to a periodic potential $U(x_j)$ and interact with each other via a pairwise potential $V(x_i-x_j)$. Equation (1) has a very broad range of interpretations; it is widely used and, depending on the choice of the parameters and the potentials, describes various physical systems. This equation has been used to describe the dynamics of an adsorbate system on a surface[2] (the linear friction coefficient is then related to the noise and the temperature via the fluctuation-dissipation theorem). In a macroscopic variation Eq. (1) describes the motion of a set of N coupled oscillators subject to a periodic potential (the Frenkel-Kontorova model; this model has been studied in relation to commensurate-incommensurate phase transitions[9]). An example of Eq. (1) applied to Hamiltonian dynamics is given in Ref. 10 and is related to energy transfer in long 1D chains adsorbed on a periodic substrate.

We study a class of models following from Eq. (1) in the absence of noise, to obtain periodic stick-slip behavior. We have developed a simple formalism to reduce the complexity of these equations and to calculate the velocity and the friction coefficient of the elements in the array for a stick-slip motion. This formalism is in good agreement with our numerical simulations and can be used for both linear and nonlinear interparticle potentials. Already in the lowest order, for which dynamics of the array can be described by an effective single-oscillator equation, our analytical predictions show very good agreement with the numerical solution.

The sliding friction coefficient strongly depends on the effective strength of the nonlinear potential (which is measured as the ratio of the time average of the nonlinear term $\partial U/\partial x$ to the time average of each one of the linear terms $\gamma\dot{x}$ or $\ddot{x}$). When this nonlinear contribution is high (for low values of the average velocity) and the dynamics of the single oscillator is more influenced by the viscosity term than by the inertia term (effectively overdamped situation), the friction coefficient $\dot{x}_{\rm av}/f$ diverges as $(\kappa-\kappa_c)^{-1/2}$ and grows linearly with the number of particles in array N; at high driving force the friction coefficient is equal to the linear friction coefficient γ (the same as for a single uncoupled oscillator).

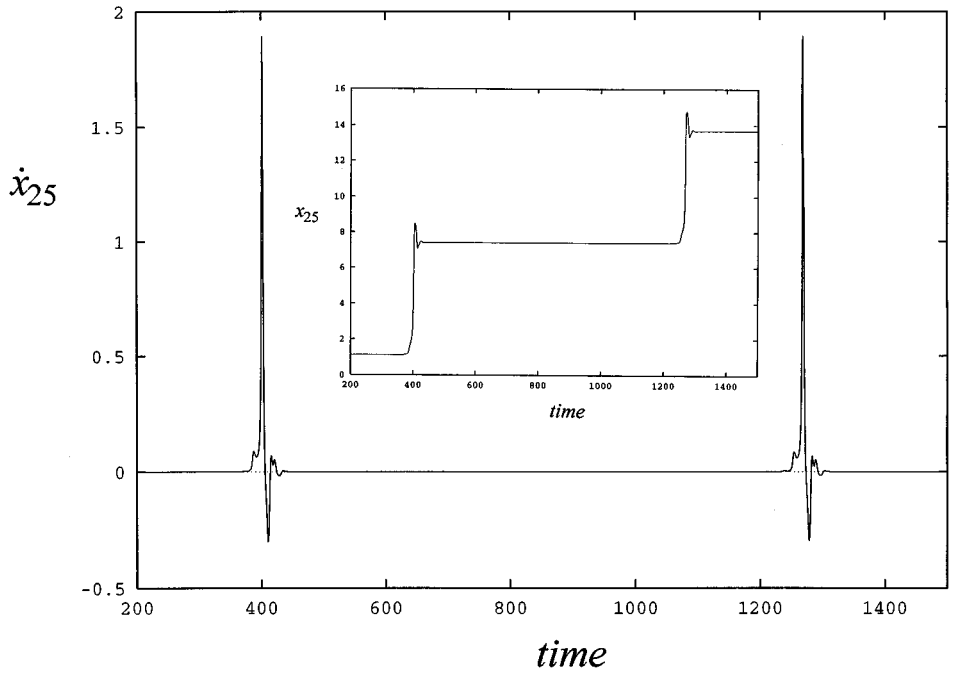

FIG. 1. Time trace of the velocity $\dot{x}_{25}$ and the position x_{25} (the inset) of the 25th oscillator of an $N=50$ oscillator array. The other parameters are $f=0.9$, $\gamma=0.7$, $\beta=0.01$, $\kappa=0.022$, and free-end boundary conditions have been imposed. The initial conditions are $x_j(0)=\dot{x}_j(0)=0$ for all $j=1,\ldots,N-1$, $x_N(0)=5$, and $\dot{x}_N(0)=0.8$.

Thus the coupling of the elements into an array, in a highly nonlinear regime, leads to a dramatic increase in the friction coefficient.

This paper is organized as follows. In Sec. II we present the theory valid in the limit of small coupling. In Sec. III we develop an approximate approach to calculate the nonlinear friction for the intermediate range of couplings. In Sec. IV we present the numerical results and compare them with our analytical predictions. A summary is given in Sec. V. Finally, our theoretical approach is expanded upon in Appendixes A and B.

II. EFFECTIVE SINGLE-OSCILLATOR DYNAMICS

We consider a variation of Eq. (1), assuming a simple periodic substrate, zero misfit length, and zero noise. Equation (1) can then be written in the dimensionless form

$$\ddot{x}_j+\gamma\dot{x}_j+F_1(x_j)=f+\frac{\kappa}{\beta}[F_2(\beta(x_{j+1}-x_j))-F_2(\beta(x_j-x_{j-1}))], \tag{2}$$

where f is the applied force (the same for all oscillators); $F_1(x_j)$ represents the periodic potential force $[F_1(x+2\pi)=F_1(x)]$, and $(\kappa/\beta)[F_2(\beta(x_{j+1}-x_j))]$ is the nearest-neighbor interaction force between the oscillators assumed to be linear at small extensions $[F_2(x)\to x$ as $x\to 0]$; κ is the nearest-neighbor coupling in the array and β is the nonlinearity parameter (β^{-1} is the range over which the nearest-neighbor coupling is effectively linear). We consider both periodic and free-end boundary conditions.

As a specific example, we will consider Morse interparticle interaction and sinusoidal substrate potential, which leads to the equations of motion

$$\ddot{x}_j+\gamma\dot{x}_j+\sin x_j=f+\frac{\kappa}{\beta}\{\exp[-\beta(x_{j+1}-x_j)]-\exp[-2\beta(x_{j+1}-x_j)]\}-\frac{\kappa}{\beta}\{\exp[-\beta(x_j-x_{j-1})]-\exp[-2\beta(x_j-x_{j-1})]\}. \tag{3}$$

As $\beta\to 0$ we obtain the linear version of Eq. (3),

$$\ddot{x}_j+\gamma\dot{x}_j+\sin x_j=f+\kappa(x_{j+1}-2x_j+x_{j-1}), \tag{4}$$

while as $\kappa=0$, the dynamics of the chain reduces to the dynamics of N uncoupled nonlinear oscillators,

$$\ddot{x}_j+\gamma\dot{x}_j+\sin x_j=f. \tag{5}$$

Equation (5) has both a ''stick'' solution $f-\sin x_{st}=0$ and a periodic ''slip'' solution $x(t)\approx\omega t+\psi(\omega t)$ [where $\psi(\omega t+2\pi)=\psi(\omega t)$].

In this section we discuss stick-slip dynamics of the chain when the coupling constant is small ($\kappa\ll 1$). We are looking for a stick-slip motion; consequently, we focus on the family of wave-propagating solutions defined by

$$x_j(t)=x(t-j\tau)+x(t+j\tau), \tag{6}$$

where τ is a characteristic time scale for slip to be propagated across the array. This kind of dynamics may occur [for instance, in Eqs. (3) and (4)] when we initially excite just one oscillator [$x_N(0)=x_0$ and $\dot{x}_N(0)=\dot{x}_0$], while all the others are initially at rest, i.e., $x_j(0)=\dot{x}_j(0)=0$, $j=1,2,3,\ldots,N-1$. The excited oscillator initiates a wave propagating across the array in a ''falling dominos'' type of motion towards the other end of the array, which is then reflected back, moving in the opposite direction towards the initially excited oscillator. To demonstrate this stick-slip motion, we present in Fig. 1 the position x_{25} and the velocity of the 25th oscillator for an array of $N=50$ oscillators interacting via

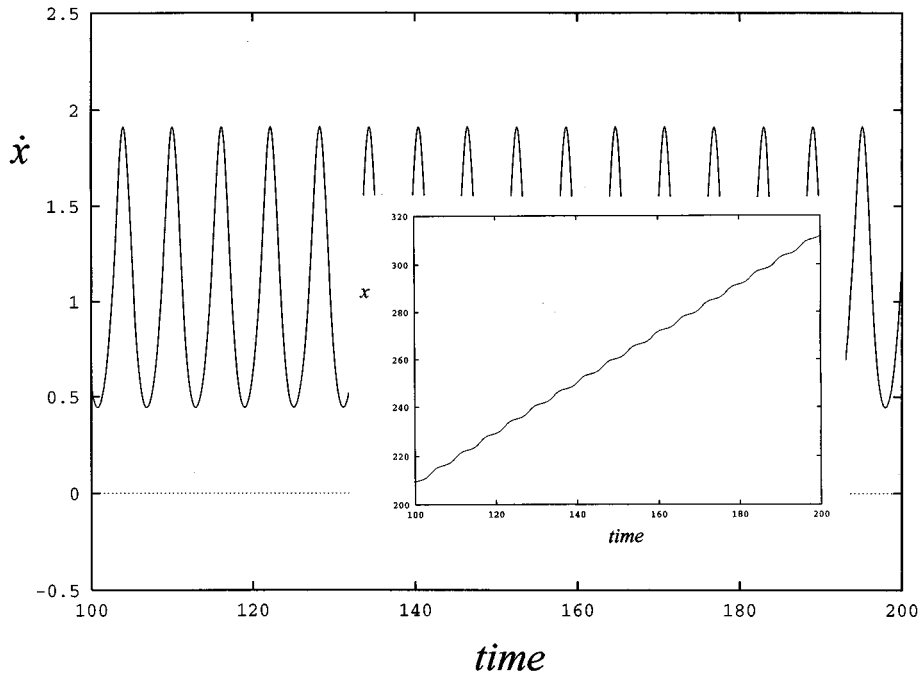

FIG. 2. Time trace of the velocity $\dot{x}_{25}$ and the position x_{25} (the inset) of the uncoupled single oscillator. The other parameters are $f=0.9$ and $\gamma=0.7$. The initial conditions are $x(0)=5$ and $\dot{x}(0)=0.8$.

nonlinear Morse potentials [Eq. (3)]. The time series (Fig. 1) clearly indicate the existence of two different types of dynamics: one that is virtually quiescent and the other one showing a fast 2π jump towards the next potential well. To contrast the dynamics of the coupled chain with that of the single uncoupled oscillator, we present in Fig. 2 time series of the position x and the velocity $\dot{x}$ of the single uncoupled oscillator (showing periodic oscillatory motion).

The stick-slip dynamics of the chain can be understood based on the following arguments [here we present an example for the sinusoidal periodic potential $F_1(x_j)=\sin x_j$]. If $f_{\min}<f<1$ ($f_{\min}$ is the minimal value of the force necessary to obtain a nonzero average velocity solution), two distinct solutions are possible, depending on initial conditions. The first is the fixed point, defined by $\sin x=f$. This solution corresponds to the static solution $v_{\rm av}=0$ when all the particles in the chain are inside their potential wells. The second solution is the limit cycle, corresponding to a running solution $v_{\rm av}>0$, where the particles hop over the potential maxima. We start with the initial conditions in which all except one of the oscillators are stuck in their potential wells and have zero velocities $[x_j(0)=\dot{x}_j(0)=0]$, while just one oscillator (the rightmost oscillator $j=N$) is given a finite displacement and a finite velocity. This right-most oscillator will initiate the motion of its neighbors in a chainlike dynamics: each oscillator will make a fast $2\pi l$ flip corresponding to a jump between l neighboring potential wells and will then stay quiescent for a long time interval.

The period of oscillations obeys, in general,

$$T_N=mN\tau, \tag{7}$$

where $m=1,2$. For periodic boundary conditions we would expect $m=1$, thus $T_N=N\tau$; for free-end boundary conditions we would expect $m=2$, thus $T_N=2N\tau$. Therefore, as the average velocity is defined by $v=\dot{x}_{\rm av}$, its value can be expressed in terms of the period T_N during which the oscillator position changes by $2\pi l$:

$$v=\frac{2\pi l}{T_N}. \tag{8}$$

The nonlinear friction coefficient η is then defined as

$$\eta=\left(\frac{f}{v}-\gamma\right)\Big/\ \gamma=\frac{fT_N}{2\pi l\gamma}-1 \tag{9}$$

to emphasize the nonlinear contribution to friction (at a high driving force we expect $\eta\to 0$). Note that since the average velocity can be expressed in terms of the characteristic time τ as

$$v=\frac{2\pi l}{mN\tau}, \tag{10}$$

then, provided the characteristic time is independent of boundary conditions, we would expect the average velocity in the presence of free-end boundary conditions to be exactly half the value for periodic boundary conditions.

We find that for given values of the external force f and the linear friction coefficient γ, there is a critical value for the coupling constant κ_c below which the linear wave [defined by Eq. (6)] will not propagate across the array. Here we will focus on the behavior of the chain in the close vicinity of this critical coupling as $\kappa\to\kappa_c$. At $\kappa=\kappa_c$ the motion is localized: at each moment effectively only one oscillator moves, driven by the force applied from its neighbors. This force can therefore be approximated to a high degree of accuracy as a constant by assuming $x_{j+1}=x_0+2\pi$ and $x_{j-1}=x_0$, where $x_0=F_1^{-1}(f)$, the stable fixed point of the single uncoupled oscillator (here we have taken $l=1$). We note that the localization of motion cannot be obtained if the linear friction coefficient γ is small enough, i.e., in underdamped situation where the effect of inertia is strong. On the other hand, the limit of overdamped dynamics ($\gamma>1$) may not lead to a stable propagating wave solution described by Eq. (6).[11] Thus, in what follows, we consider the case of

effectively overdamped array where there exist stable linear wave solution [Eq. (6)] and the damping coefficient of each single oscillator is high enough to ensure the localization of motion in the vicinity of $\kappa \approx \kappa_c$.[12]

We have developed[13] an n-cluster approximation to solve the equations [Eq. (2)], which can be applicable for the kind of dynamics described above. The main idea in our approach is that n coupled oscillators are treated as being in the presence of a force generated by the remaining quiescent oscillators assumed to take the values $x_{\text{right}}=x_0+2\pi$ and $x_{\text{left}}=x_0$ [$x_0=F_1^{-1}(f)$], representing a traveling wave moving through the array from right to left. In the lowest-order approximation ($n=1$) we obtain

$$\ddot{x}+\gamma\dot{x}+F_1(x)=f+\frac{\kappa}{\beta}[F_2(\beta(x_0+2\pi-x)) - F_2(\beta(x-x_0))]. \tag{11}$$

The characteristic time τ for the excitation to pass between oscillators (a property of the array) can be approximated here by $\tau=T$, where T is the time each oscillator moves separately. Therefore, τ and consequently the average velocity can be calculated using Eq. (11) together with the matching initial conditions

$$x(0)=F_1^{-1}(f)=x_0, \tag{12a}$$

$$\dot{x}(0)=0. \tag{12b}$$

To find T we integrate Eq. (11). The details of the calculation are presented in Appendix A. The resulting expression is

$$T=\gamma\sqrt{\frac{2\pi}{F''(x_c,\kappa_c)\partial F(x_c,\kappa_c)/\partial\kappa}}\,[\kappa-\kappa_c(f,\beta)]^{-1/2}, \tag{13}$$

where

$$F=f-F_1(x)+\frac{\kappa}{\beta}[F_2(\beta(x_0+2\pi-x))-F_2(\beta(x-x_0))] \tag{14}$$

and x_c and κ_c are the critical values of the displacement and the coupling determined by the instability of the fixed point solution [see Appendix A, Eq. (A8)]. Equation (13) can be used to calculate the average velocity v [Eq. (8)] and the average nonlinear friction coefficient η [Eq. (9)] for a variety of nonlinear potentials and nearest-neighbor couplings.

For example, for linear coupling and a sinusoidal periodic potential to a good approximation, as $\kappa\to\kappa_c$ this time period is[14]

$$T\approx\gamma\sqrt{\frac{\pi}{\pi-\cos^{-1}f}}\,(\kappa-\kappa_c)^{-1/2}, \tag{15}$$

where $\kappa_c\approx(1-f)/2\pi+O((1-f)^2)$. Equations (10) and (15) lead to the following expression for the velocity of the chain:

$$v=\frac{2\pi l}{mN\gamma}\sqrt{\frac{\pi-\cos^{-1}f}{\pi}}\,(\kappa-\kappa_c)^{1/2}, \tag{16}$$

and, in the leading order, the average velocity scales as $(\kappa-\kappa_c)^{1/2}$. Consequently, the nonlinear friction coefficient η diverges as $(\kappa-\kappa_c)^{-1/2}$ and is given by the expression

$$\eta=\frac{mNf}{2\pi l}\sqrt{\frac{\pi}{\pi-\cos^{-1}f}}\,(\kappa-\kappa_c)^{-1/2}-1. \tag{17}$$

Next consider the nonlinear Morse interaction potential and the sinusoidal substrate [Eq. (3)]. In this case $F_1(x)=\sin x$ and $F_2(x)=\exp(-x)-\exp(-2x)$, and using Eqs. (13) and (14) we can find an expression for the period of the oscillations. We need to calculate $F''(x_c,\kappa_c)$ and $\partial F(x_c,\kappa_c)/\partial\kappa$ for the Morse potential and these are given by Eqs. (A26) of Appendix A.

The main effect of the nonlinearity in the interaction β is to shift the critical value of $\kappa_c(\beta)$ upward [the lowest-order correction is given by Eq. (A30) for the Morse potential] and in consequence for very small β ($2\pi\beta\ll 1$), $\tau(\beta)$ increases with β as $\tau(\beta)\approx\tau_l(1+A\beta)$; here A is a constant and τ_l is the value of τ derived for the linear interparticle interaction [Eq. (15)]. As β increases further, it will approach a critical value β_c given by the implicit equation $\kappa_c(\beta_c)=\kappa$ at which this time scale diverges. The most singular contribution of the nonlinearity β to the scale separation period τ, in the vicinity of β_c, is then given by [see Eq. (A36)]

$$\tau(\beta)\approx\tau(\beta_c)[(\beta_c-\beta)/\beta_c]^{-1/2}, \tag{18}$$

where $\tau(\beta_c)$ is a constant and β_c is the value of β at which the period diverges. Because of the close relationship between the period and the nonlinear friction η we also find that, as $\beta\to\beta_c$, its most singular term may be expected to diverge as

$$\eta(\beta)\approx\eta(\beta_c)[(\beta_c-\beta)/\beta_c]^{-1/2}. \tag{19}$$

Equations (17) and (19) indicate a dramatic increase in the friction coefficient of an array compared to the friction coefficient of a single uncoupled oscillator, even though the same constant force is applied to each oscillator in the array. Also note that (as $\kappa\to\kappa_c$) the friction coefficient is proportional to the size of the chain $\eta\propto N$.

By manipulating initial conditions, different solutions are obtained. In particular, we have found a family of solutions corresponding to harmonic and subharmonic ratios of the minimal velocity v_0 [Eq. (8), $l=1$], $v=(k/m)v_0$. Figure 3(a) demonstrates the situation where the average velocity is twice the minimal average velocity v_0. Figure 3(b) shows the case when the average velocity is three times the minimal average velocity v_0.

The formalism developed in this section is strictly valid only for $\kappa\to\kappa_c$, though the agreement between the numerical simulations and the theoretical predictions extends for values of κ far beyond the value of κ_c. In the next section we present the analysis for the situation where $\kappa\gg\kappa_c$.

III. ANALYTICAL RESULTS: INTERMEDIATE-COUPLING RANGE

In this section we study the dynamics of the linear chain in the range of intermediate coupling $\kappa\gg\kappa_c$. In contrast to the limit of $\kappa\approx\kappa_c$ where at any given time only one oscillator moves and there exists localization of motion in time, here

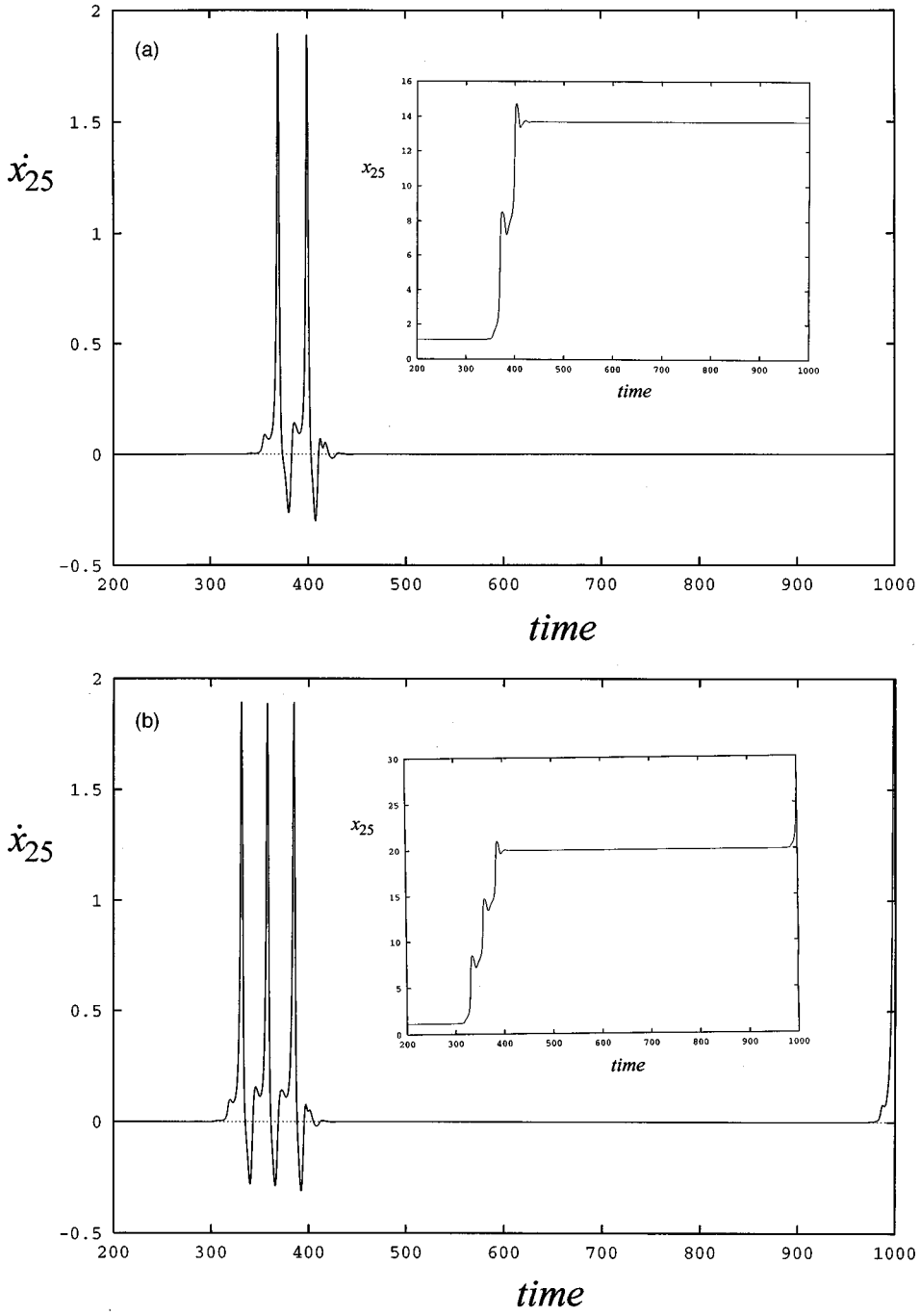

FIG. 3. Time trace of the velocity $\dot{x}_{25}$ and the position x_{25} (the inset) of the 25th oscillator of an $N=50$ oscillator array. The other parameters are $f=0.9$, $\gamma=0.7$, $\beta=0.01$, $\kappa=0.022$, and free-end boundary conditions. The initial conditions are $x_j(0)=\dot{x}_j(0)=0$ for all $j=1,\ldots,N-2$, $x_N(0)=x_{N-1}(0)=5$, and $\dot{x}_N(0)=\dot{x}_{N-1}(0)=0.8$. (b) Same as (a), but with $x_{N-2}(0)=5$ and $\dot{x}_{N-2}(0)=0.8$.

we study the case when the motion is not localized, and therefore a large cluster of oscillators moves at the same time. This type of dynamics occurs at $\kappa \approx O(1)$. The strength of coupling introduces very important effects into the dynamics of the chain. When the coupling is strong enough, the ''barrier crossing'' time of a single oscillator $T \equiv 2\pi/\omega$ is compatible with the period of motion of the whole array T_N and the separation time τ [see Eq. (6)] is much less than T ($\tau \ll T$). In contrast, for the case of weak coupling $T_N \approx TN$ and $\tau \approx T$, for the intermediate-coupling case we have $T < T_N < TN$ and $\tau < T$. An example of the time series for the position and the velocity of the 25th oscillator in an array of $N=50$ oscillators is shown in Fig. 4.

Our starting point is to combine Eqs. (4) and (6) to derive the effective single-oscillator equation

$$\ddot{x}_j + \gamma \dot{x}_j + \sin x_j = f + 2\kappa(\cosh \tau d/dt - 1)x_j . \tag{20}$$

In deriving Eq. (20) we used the identity $x(t \pm \tau) = e^{\pm \tau d/dt} x(t)$. We use our knowledge of the dynamics to seek an approximate form for the solution. For times $(0 < t < T \equiv 2\pi/\omega)$ during which the running solution exists we approximate the motion of the oscillator by the ansatz

$$x(t) = A + \omega t + \sum_{k=1}^{\infty} B_k \sin(k\omega t + \beta_k). \tag{21}$$

For the rest of the time $(2\pi/\omega < t < T_N \equiv 2\pi/v)$ $x(t) = \sin^{-1} f$ (v is the average velocity of the chain). Note that Eq. (21) represents the expansion of $x(t) = \omega t + \xi(\omega t)$, where $\xi(x) = \xi(x + 2\pi)$ is a periodic function in a Fourier

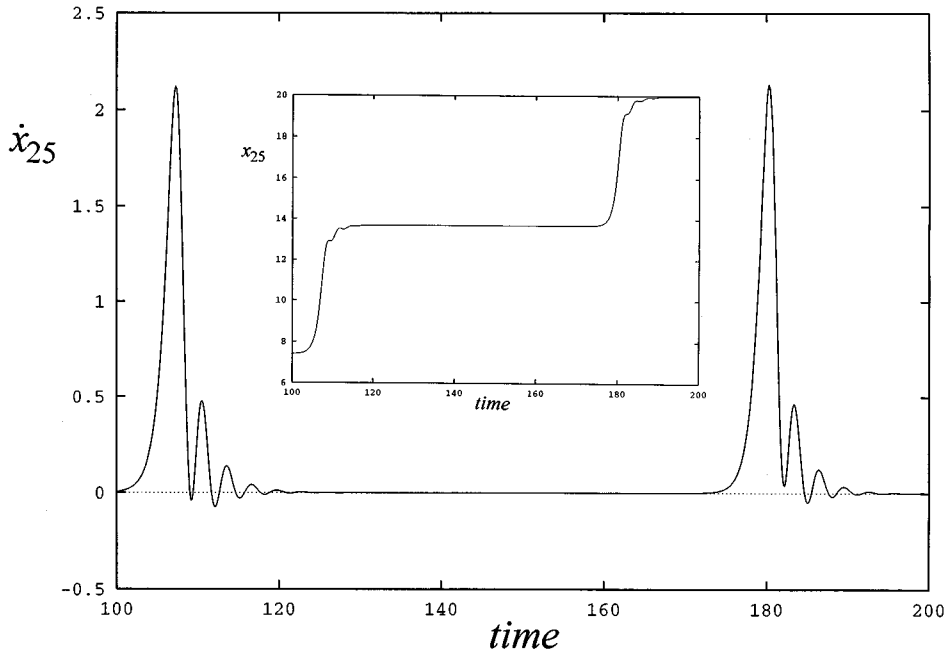

FIG. 4. Time trace of the velocity $\dot{x}_{25}$ and the position x_{25} (the inset) of the 25th oscillator of an $N=50$ oscillator array. The other parameters are $f=0.9$, $\gamma=0.7$, $\beta=0.01$, $\kappa=0.9$, and free-end boundary conditions. The initial conditions are $x_j(0)=\dot{x}_j(0)=0$ for all $j=1,\ldots,N-1$, $x_N(0)=5$, and $\dot{x}_N(0)=0.8$.

series. In the equations of motion [Eq. (4)] every single oscillator j is influenced by its nearest neighbors $j+1$ and $j-1$. Since for times $0<t<2\pi/\omega$ the oscillators j, $j+1$, and $j-1$ all move, we substitute the ansatz (21) into Eq. (20) (to describe the dynamics of the oscillator j), which leads to the expression

$$-\omega^2\sum_{k=1}^{\infty} k^2 B_k \sin(k\omega t+\beta_k)+\gamma\omega\sum_{k=1}^{\infty} kB_k\cos(k\omega t+\beta_k)$$
$$+\sin\left[(A-\beta_1)+(\omega t+\beta_1)+\sum_{k=1}^{\infty} B_k\sin(k\omega t+\beta_k)\right]$$
$$=f-\gamma\omega-4\kappa\sum_{k=1}^{\infty} B_k\sin(k\omega t+\beta_k)\sin^2\frac{\pi l\omega k}{mNv}. \qquad (22)$$

Let us rewrite Eq. (22) in the form

$$-\omega^2\sum_{k=1}^{\infty} k^2 B_k \sin(k\omega t+\beta_k)+\gamma\omega\sum_{k=1}^{\infty} kB_k\cos(k\omega t+\beta_k)$$
$$+\sum_{k=0}^{\infty} g_k(A,\{B\},\{\beta\})B_k\cos(k\omega t+\beta_k)$$
$$+\sum_{k=1}^{\infty} f_k(A,\{B\},\{\beta\})B_k\sin(k\omega t+\beta_k)$$
$$=f-\gamma\omega-4\kappa\sum_{k=1}^{\infty} B_k\sin(k\omega t+\beta_k)\sin^2\frac{\pi l\omega k}{mNv}. \qquad (23)$$

The functions f_k and g_k depend, in general, on A and the complete set of amplitudes $\{B\}$ and phases $\{\beta\}$, which appear in the form of Bessel functions $J_n(B_i)$ and in the cross terms of the form $J_n(B_i)J_m(B_j)$. Equation (23) can be now written as a set of equations

$$g_0(A,\{B\},\{\beta\})=f-\gamma\omega, \qquad (24a)$$

$$k\gamma\omega+g_k(A,\{B\},\{\beta\})=0, \qquad (24b)$$

$$-k^2\omega^2+f_k(A,\{B\},\{\beta\})=-4\kappa\sin^2\frac{\pi l\omega k}{mNv}. \qquad (24c)$$

Though Eqs. (24) are intractable without severe truncation, some general features can be gleaned from their structure. In the limit of weak coupling a perturbative solution appears to exist in which the amplitudes $A,\{B\}$ and the phases $\{\beta\}$ can be solved for in the $\kappa=0$ limit and then substituted into the equations for the velocity v. Thus, for small enough κ the main features of the dynamics of the barrier crossing at times $0<t<2\pi/\omega$ do not depend strongly on the parameters of the chain N and κ [this ansatz had been successfully tested numerically for $\kappa\approx O(1)$ as well]; if $\pi l\omega k/mNv$ is small enough that the approximation $\sin x\approx x$ is reasonable, the average velocity is given by

$$v\approx\frac{\sqrt{\kappa}}{N}G(f,\gamma). \qquad (25)$$

The condition $\pi l\omega k/mNv<1$ occurs in situations where many oscillators move at the same time (opposite to the situation near $\kappa\approx\kappa_c$, where only one oscillator moves at a given time), thus the barrier crossing time of one oscillator $T=2\pi/\omega$ is compatible with the period of the whole array T_N. We performed numerical tests to verify this condition and found that the approximation $\sin x\approx x$ is fair for such dynamics. We also tested numerically the expression [Eq. (25)] in the range of $1<\kappa<3$ for $N=25$ oscillator array and found that the average velocity $v\propto\kappa^{0.48}$, which is in good agreement with the prediction of Eq. (25).

To test the predictions of Eq. (25), we performed an analysis using just the first harmonic in the expansion of Eqs. (24) expressing the position of the oscillator during the period $0<t<T\equiv 2\pi/\omega$ as

$$x(t)=A+\omega t+B\sin(\omega t+\beta), \qquad (26)$$

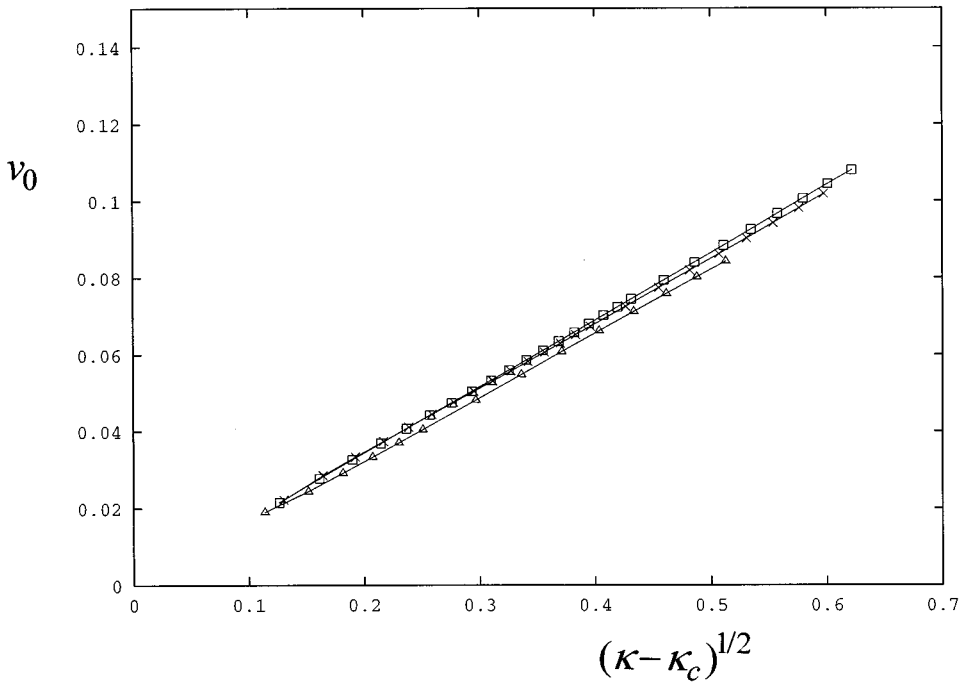

FIG. 5. Time-averaged minimal velocities of the oscillators v_0 as a function of $(\kappa-\kappa_c)^{1/2}$ for $N=25$ and three different values of $\beta=0.01,0.1,0.2$ (from top to bottom). The squares ($\beta=0.01$), crosses ($\beta=0.1$), and triangles ($\beta=0.2$) denote numerically calculated values of the average velocity, while the lines are to guide the eye. The other parameters are the same as in Fig. 1 and $\kappa=0.05$. The initial conditions are $x_N(0)=5$, $\dot{x}_N(0)=0.8$, and $x_j(0)=\dot{x}_j(0)=0$ for all $j=1,\ldots,N-1$.

where ω is the characteristic overturning frequency of each single oscillator. During the rest of the period $T\equiv 2\pi/\omega<t<T_N$ (which forms a stick phase), $x=\sin^{-1}f$. The details of the calculations are presented in Appendix B. Here we present the main expression

$$\mathcal{F}(f,\gamma)\equiv\frac{\Omega^2(f)}{\gamma^2}+G(f)=4\kappa\,\sin^2\frac{\pi l\Omega(f)}{\gamma mNv}, \quad (27)$$

where the functions $\Omega(f),G(f)$ are given by Eqs. (B11) and (B13).

For small enough $\pi l\Omega/\gamma mNv$ one can approximate Eq. (27) as

$$\sqrt{\mathcal{F}(f,\gamma)}\approx 2\pi l\sqrt{\kappa}\,\frac{\Omega(f)}{\gamma mNv}, \quad (28)$$

and the average velocity is then given in this limit by

$$v\approx\frac{2\pi l\sqrt{\kappa}}{mN}\,\frac{\Omega(f)}{\gamma\sqrt{\mathcal{F}(f,\gamma)}}. \quad (29)$$

A comparison of Eqs. (29) and (15) suggests that $\Omega(f)/\gamma\sqrt{\mathcal{F}(f,\gamma)}\to\sqrt{(\pi-\cos^{-1}f)/\pi}$ as $f\to 1$.

Specifically it is clear from Eq. (29) that for the range of intermediate values of the coupling constant and for the forcing $f<1$ (where the dynamics of the array cannot be described by continuum limit of sine-Gordon equation[15]) the average velocity is proportional to the square root of the coupling $v\propto\sqrt{\kappa}$, which is in good agreement with our simulations. The actual values of the average velocity (obtained from our numerical simulations for intermediate values of the coupling κ and for the other parameter values as in Fig. 5) are higher by 20–30 % from the predicted values [Eq. (29)]. This discrepancy is (mainly) due to the simplified description of the position [Eq. (26)] keeping only the first harmonic in the expansion [Eq. (21)]. It is also clear [from the structure of Eq. (27)] that there is a minimum value of κ for which a solution exists,

$$\kappa_c=\frac{\mathcal{F}(f,\gamma)}{4}, \quad (30)$$

and the comparison of this result with the values of κ_c estimated in Sec. II suggests that $\mathcal{F}(f,\gamma)\to 2(1-f)/\pi$ as $f\to 1$.

IV. NUMERICAL RESULTS

We solved Eq. (3) numerically using arrays containing $N=18$, 25, 35, 42, and 50 oscillators. The external force was set to $f=0.9$ and the dissipation $\gamma=0.7$; the coupling constant κ varied from 0 to 1, while the nonlinearity parameter β went from 0.01 to 0.25. Simulations were carried out for both periodic and free-end boundary conditions.

In Fig. 5 we have plotted the average velocity of the oscillators as a function of the coupling constant $(\kappa-\kappa_c)^{1/2}$ for $N=25$ and $\beta=0.01,0.1,0.2$; we were using the same single-oscillator parameters $f=0.9$ and $\gamma=0.7$, and free-end initial conditions were imposed. (The numerically calculated average velocities for periodic boundary conditions are roughly twice as large as those for free-end initial conditions, as predicted by analytical considerations [Eq. (16)].) The initial conditions were chosen in the following way: $x_N=5$ and $\dot{x}_N=0.8$; the other oscillators were set initially with $x_j=\dot{x}_j=0$.

The solid lines in Fig. 5 are to guide the eye, while the points show the numerical values. The values of κ have been varied between 0 and 0.4, and κ_c was estimated from the numerical simulations. All curves show the $(\kappa-\kappa_c)^{1/2}$ behavior; the larger slopes correspond to smaller-β values. This behavior agrees with our prediction that the effect of the nonlinearity in the interaction β is to increase κ_c and, consequently, to decrease the average velocity of motion (for a

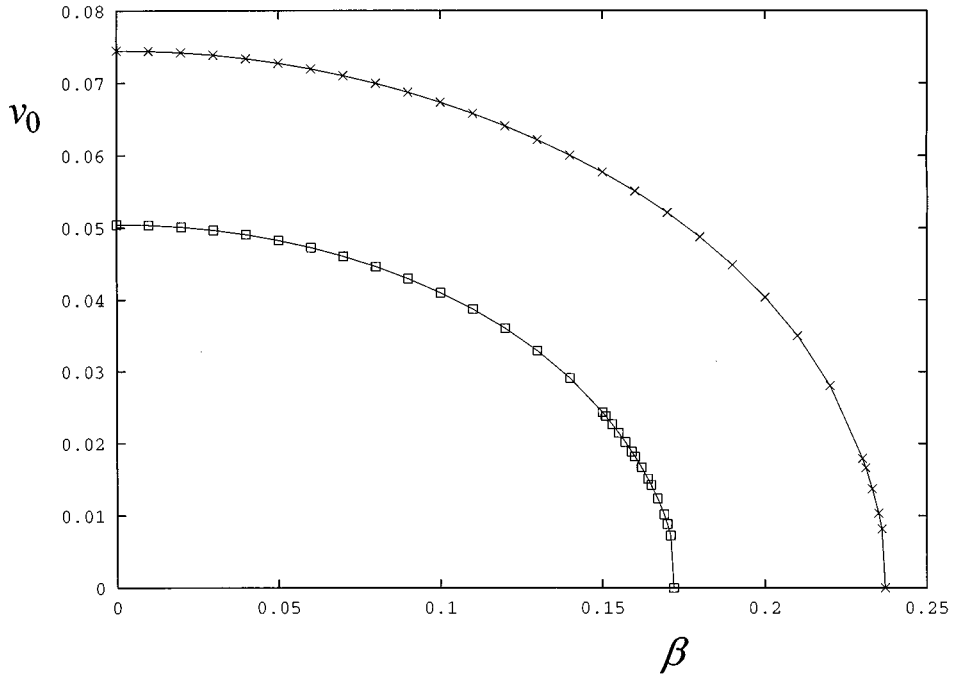

FIG. 6. Time-averaged minimal velocity of the oscillators as a function of the nonlinearity parameter β for an $N=25$ oscillators array. The crosses (top curve) are the numerically calculated values for $\kappa=0.2$, while the squares (bottom curve) correspond to $\kappa=0.1$; the lines are to guide the eye. The other parameters are $f=0.9$ and $\gamma=0.7$.

given value of the coupling κ). We found that in a very narrow range of κ there exists an in-phase solution of the array (not shown in Fig. 5), resulting in a high average velocity of a chain (equal to the average velocity of uncoupled oscillator). This resonance is also predicted by the equation for a single oscillator [Eq. (A2)]. The in-phase solution then disappears, leading to stick-slip motion of the oscillators.

Figure 6 shows the numerically calculated minimal value of the average velocity v_0 as a function of the nonlinearity parameter β, when β varies from 0 to β_c. In the vicinity of β_c [Eq. (19)] the slope is approximately $\frac{1}{2}$, while for small β $[v_0(\beta)\approx v_l(1-A\beta)]$, A is a constant.

Figure 7 shows the nonlinear friction coefficient η of the array as a function of applied force f for $\kappa=0.1$ and $\beta=0.01$ and 0.05 [compare to Eq. (19)]. Each point on the curve was calculated using the same set of initial conditions for each value of the external force f (see Fig. 1). The curve shows the presence of two dynamical transitions at f_{c1} and f_{c2} and its resulting effect on the average value of the sliding friction. If the external force is low $f_{\min}<f<f_{c1}$, the dynamics of an array shows stick-slip motion. As we increase the force, the array undergoes a dynamical transition at f_{c1} to a different kind of dynamics, valid for forcing in the range $f_{c1}<f<f_{c2}$, where the oscillators form two separate clusters consisting of alternate oscillators, the oscillators in each cluster being almost in phase, but out of phase with the oscilla-

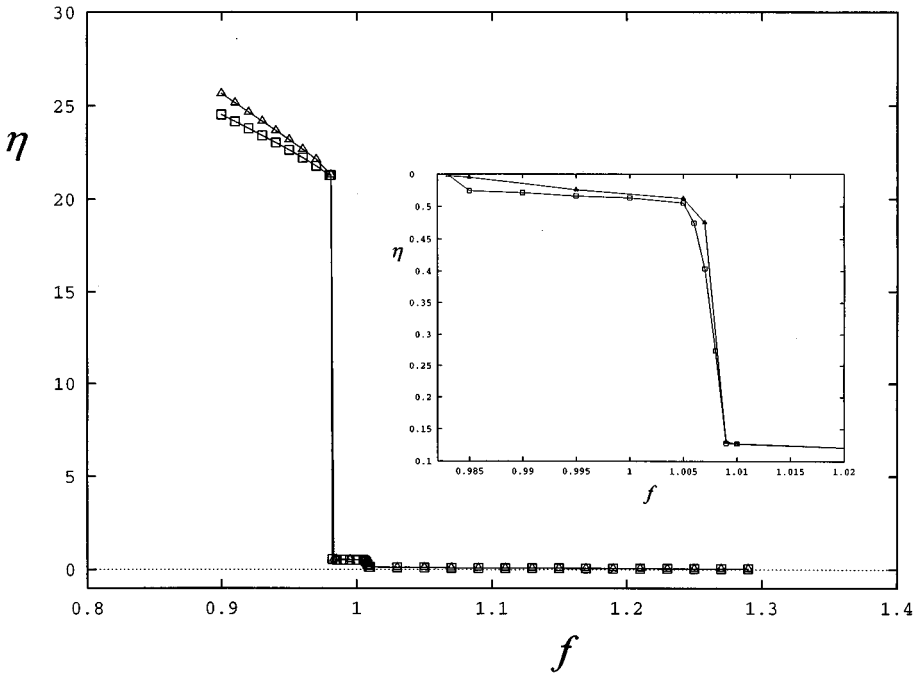

FIG. 7. Friction coefficient $\eta=(f/v_0-\gamma)/\gamma$ as a function of the applied force f for an $N=25$ oscillator array. The triangles (top curve) correspond to $\beta=0.05$, while the squares (bottom curve) correspond to $\beta=0.01$ and free-end boundary conditions. The lines plotted are to guide the eye. The other parameters are the same as in Fig. 1 and $\kappa=0.05$. The inset shows the small region of the same plot to mark the differences between these two curves.

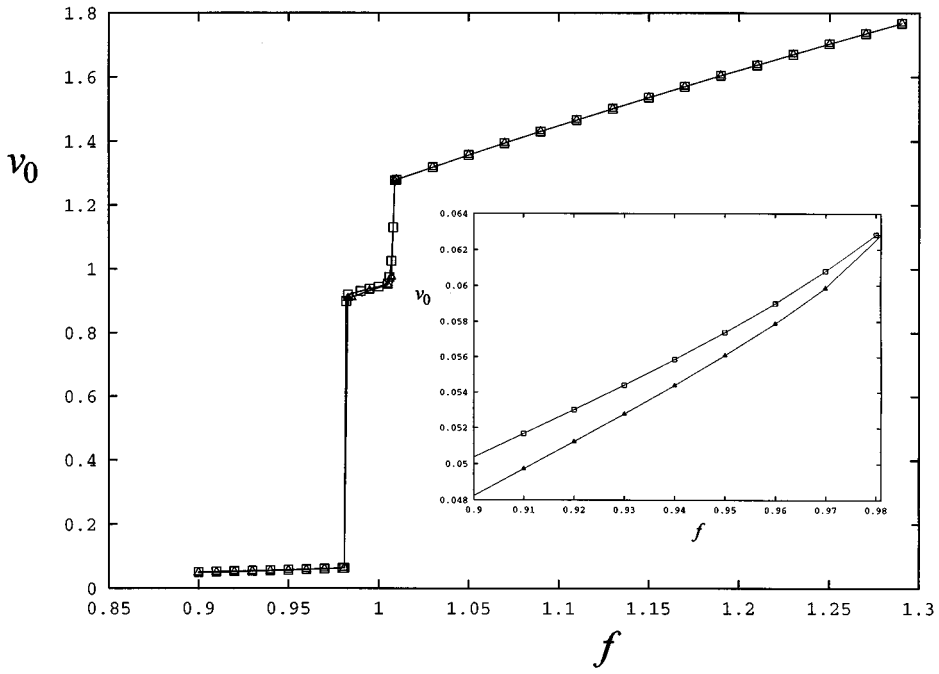

FIG. 8. Minimal velocity v_0 as a function of the applied force f for an $N=25$ oscillator arrays. The squares (top curve) correspond to $\beta=0.01$, while the triangles (bottom curve) correspond to $\beta=0.05$ and free-end boundary conditions. The lines plotted are to guide the eye. The other parameters are the same as in Fig. 1 and $\kappa=0.05$. The inset shows the small region of the same plot to mark the differences between these two curves.

tors forming the other cluster. Finally, for even larger external forces $f>f_{c2}$, the dynamics is the stable ''in-phase'' solution and all the oscillators move together. Figure 8 shows the minimal average velocity v_0 as a function of the applied force.

V. SUMMARY

We have studied the periodic stick-slip dynamics in a class of nearest-neighbor interacting discrete chains of coupled nonlinear oscillators subject to a periodic potential. We identified the mechanism of stick-slip motion, which is related to the periodic transition from a stick dynamics characterized by the stable fixed point of the single uncoupled oscillator (in which each particle forming the chain is stuck in its potential well) to slip motion corresponding to the limit cycle of the oscillator due to its motion over the periodic potential. The nonlinear dynamics leads to a fundamentally different friction law, in particular when the driving force is barely larger than the minimal force needed to start motion. The friction coefficient grows with the number of elements N in the array and for effectively overdamped dynamics scales as $(\kappa-\kappa_c)^{-1/2}$. Similarly, the average velocity, as calculated from Eq. (16), exhibits the $(\kappa-\kappa_c)^{1/2}$ dependence. The nonlinearity in interaction provides an additional source for the increase in friction coefficient; in the vicinity of β_c, $\eta \propto \eta_l[(\beta_c-\beta)/\beta_c]^{-1/2}$. Our predictions are in excellent agreement with the numerically calculated values.

ACKNOWLEDGMENTS

This work was partially supported by the National Science Foundation and the Office of Naval Research. We thank Professor B. Titus for his helpful comments in reading the manuscript.

APPENDIX A

In this section we derive the expressions for the period of the oscillations T. Our starting point is

$$\ddot{x}_j+\gamma\dot{x}_j+F_1(x_j)=f+\frac{\kappa}{\beta}[F_2(\beta(x_{j+1}-x_j)) - F_2(\beta(x_j-x_{j-1}))], \tag{A1}$$

where $F_1(x+2\pi)=F_1(2\pi)$ and $F_2(x)\to x$ as $x\to 0$. The next step is to decouple these equations (in the limit of very small coupling κ), so that $x_j=x$, $x_{j+1}=x_0+2\pi$, and $x_{j-1}=x_0$; here $x_0=F_1^{-1}(f)$, the fixed point of the uncoupled oscillator. Thus Eq. (A1) can be written as

$$\ddot{x}+\gamma\dot{x}+F_1(x)=f+\frac{\kappa}{\beta}[F_2(\beta(x_0+2\pi-x)) - F_2(\beta(x-x_0))]. \tag{A2}$$

Let us rewrite Eq. (A2) in the form

$$\dot{x}=y, \quad \dot{y}=-\gamma y+F(x,f,\beta,\kappa), \tag{A3}$$

where

$$F=f-F_1(x)+\frac{\kappa}{\beta}[F_2(\beta(x_0+2\pi-x))-F_2(\beta(x-x_0))]. \tag{A4}$$

The fixed point ($x=x_c$, $y=0$), where x_c is given by the implicit equation $F(x_c,f,\beta,\kappa)=0$, becomes unstable when the eigenvalues λ of the linearized equation

$$\delta\dot{x}=y,$$

$$\dot{y}=-\gamma y+F'\delta x, \tag{A5}$$

where $F'=\partial F(x_c,f,\beta,\kappa)/\partial x_c$ becomes positive ($\lambda>0$).

The equation for λ is

$$\lambda^2+\gamma\lambda-F'=0, \tag{A6}$$

which can be solved to give

$$\lambda=\frac{-\gamma\pm\sqrt{\gamma^2+4F'}}{2}. \tag{A7}$$

Thus, for $F'<0$ we get an attractor, while for $F'>0$, a saddle point occurs. A traveling wave can thus propagate through the array when $\kappa>\kappa_c$ given by

$$F(x_c,f,\beta,\kappa_c)=0, \quad F'(x_c,f,\beta,\kappa_c)=0. \tag{A8}$$

As $\kappa\to\kappa_c$, we may expand F about x_c and κ_c and represent it by the universal form

$$F(x,f,\beta,\kappa)=\frac{1}{2}F''(x-x_c)^2+\frac{\partial F}{\partial\kappa}(\kappa-\kappa_c), \tag{A9}$$

which will control the dynamics. Neglecting the inertial term $\ddot{x}$ compared to the dissipative contribution $\gamma\dot{x}$ as $\kappa\to\kappa_c$, which we justify *a posteriori* because

$$\frac{\ddot{x}}{\gamma\dot{x}}\approx\frac{T}{T^2\gamma}\approx\frac{1}{\gamma T}\sim\frac{(\kappa-\kappa_c)^{1/2}}{\gamma}, \tag{A10}$$

we can find T from the equation

$$\gamma\dot{x}=F(x,f,\beta,\kappa) \tag{A11}$$

or

$$\int\frac{dx}{F}=\int\frac{dt}{\gamma}=\frac{T}{\gamma}=\int dx\,\exp(-\ln F), \tag{A12}$$

which we can integrate using saddle-point integration about x_c. In this region,

$$\ln(F)\approx\ln F(x_c)+\frac{F'}{F}(x-x_c)+\frac{FF''-F'^2}{2F^2}(x-x_c)^2, \tag{A13}$$

but as $F'(x_c)=0$ we find

$$\ln(F)\approx\ln F(x_c)+\frac{F''(x_c)}{2F(x_c)}(x-x_c)^2. \tag{A14}$$

Thus, for κ close to κ_c we obtain

$$\frac{T}{\gamma}\approx F^{-1}(x_c,\kappa_c)\int_{-\infty}^{\infty}\exp-\left(\frac{F''(x_c)}{2F(x_c)}(x-x_c)^2\right)dx \tag{A15}$$

or

$$\frac{T}{\gamma}\approx F^{-1}\sqrt{\frac{2\pi F}{F''}}=\sqrt{2\pi/FF''}, \tag{A16}$$

and, finally,

$$T=\gamma\sqrt{\frac{2\pi}{F''(x_c,\kappa_c)\partial F(x_c,\kappa_c)/\partial\kappa}}\,[\kappa-\kappa_c(f,\beta)]^{-1/2}. \tag{A17}$$

Now we can apply the results to specific examples. Our first example is the linear chain subject to a sinusoidal periodic potential; thus $F_1(x)=\sin x$ and $F=f-\sin x+2\kappa(\pi+x_0-x)$, where $\sin x_0=f$. Thus $\kappa_c(f)$ and $x_c(f)$ can be found from

$$F=f-\sin(x_c)+2\kappa(x_0+\pi-x_c)=0.$$

$$\frac{\partial F}{\partial x}=-\cos x_c-2\kappa_c=0. \tag{A18}$$

Also, since

$$F''(x_c,\kappa_c)=\sin(x_c),$$

$$\frac{\partial F(x_c,\kappa_c)}{\partial\kappa}=2(\pi+x_0-x_c), \tag{A19}$$

we find

$$T=\gamma\sqrt{\frac{\pi}{\sin x_c(\pi+x_0-x_c)}}\,[\kappa-\kappa_c(f,\beta)]^{-1/2}, \tag{A20}$$

where $x_0=\sin^{-1}(f)$ and $\cos x_c=-2\kappa_c$. We can therefore rewrite Eq. (A20), using $\sin x_c=\sqrt{1-4\kappa_c^2}$, as

$$x_c=\frac{\pi}{2}+\sin^{-1}(2\kappa_c); \tag{A21}$$

thus

$$T=\gamma\sqrt{\frac{\pi}{\sqrt{1-4\kappa_c^2}[\pi-\cos^{-1}(f)-\sin^{-1}(2\kappa_c)]}}\times(\kappa-\kappa_c)^{-1/2}; \tag{A22}$$

For $\kappa_c\ll 1$, Eq. (A22) simplifies to

$$T=\gamma\sqrt{\frac{\pi}{\pi-\cos^{-1}(f)}}\,(\kappa-\kappa_c)^{-1/2}. \tag{A23}$$

Our next example is a Morse interaction for which $F_2(x)=\exp(-x)-\exp(-2x)$. In this case

$$F=f-\sin x+\frac{\kappa}{\beta}\{\exp[-\beta(x_0+2\pi-x)]-\exp[-2\beta(x_0+2\pi-x)]\}-\frac{\kappa}{\beta}\{\exp[-\beta(x-x_0)]-\exp[-2\beta(x-x_0)]\}. \tag{A24}$$

Thus $\kappa_c(f,\beta)$ and $x_c(f,\beta)$ can be found from

$$F=f-\sin x_c+\frac{\kappa}{\beta}\{\exp[-\beta(x_0+2\pi-x_c)]-\exp[-2\beta(x_0+2\pi-x_c)]\}-\frac{\kappa}{\beta}\{\exp[-\beta(x_c-x_0)]-\exp[-2\beta(x_c-x_0)]\}=0, \tag{A25}$$

$$\frac{\partial F}{\partial x} = -\cos(x_c) - \kappa\{\exp[-\beta(x_0+2\pi-x_c)] - \exp[-2\beta(x_0+2\pi-x_c)]\} + \kappa\{\exp[-\beta(x_c-x_0)] - \exp[-2\beta(x_c-x_0)]\} = 0,$$

and then the period is given by Eq. (A17) with

$$\begin{aligned} F''(x_c,\kappa_c) &= \sin x_c + \kappa\beta\{\exp[-\beta(x_0+2\pi-x_c)] - 4\exp[-2\beta(x_0+2\pi-x_c)]\} \\ &\quad - \frac{\kappa}{\beta}\{\exp[-\beta(x_c-x_0)] - 4\exp[-2\beta(x_c-x_0)]\}, \\ \partial F(x_c,\kappa_c)/\partial\kappa &= 1/\beta\{\exp[-\beta(x_0+2\pi-x_c)] - \exp[-2\beta(x_0+2\pi-x_c)]\} \\ &\quad - 1/\beta\{\exp[-\beta(x_c-x_0)] - \exp[-2\beta(x_c-x_0)]\}. \end{aligned} \tag{A26}$$

Because of the complexity of these expressions it is useful to solve for $\beta \ll 1$ by introducing a perturbation solution for $F(x_c,f,\beta,\kappa_c)=0$ and $\partial F(x_c,f,\beta,\kappa_c)/\partial x = 0$,

$$\begin{aligned} F &= F^l + F^1\beta + \cdots, \\ x_c &= x_l + x_1\beta + \cdots \\ \kappa_c &= \kappa_l + \kappa_1\beta + \cdots, \end{aligned} \tag{A27}$$

where x_l and κ_l are the solutions of the linear array $F^l(x_l,f,\kappa_l)=0$ and $\partial F^l(x_l,f,\kappa_l)/\partial x = 0$. For κ_1 we then find the expression

$$\kappa_1 = -F^1(x_l,f,\kappa_l) \Big/ \frac{\partial F^l(x_l,f,\kappa_1)}{\partial\kappa}. \tag{A28}$$

Now, in general, we may write

$$\begin{aligned} F^1 &= -F_2''(0)\,\frac{\kappa_l}{2}\,[(x_0+2\pi-x_l)^2-(x_l-x_0)^2], \\ \frac{\partial F^l}{\partial\kappa} &= 2(\pi+x_0-x_l); \end{aligned} \tag{A29}$$

therefore, for the Morse potential

$$\kappa_1 = \frac{3\kappa_l}{4}\,\frac{[(x_0+2\pi-x_l)^2-(x_l-x_0)^2]}{(\pi+x_0-x_l)^2} \tag{A30}$$

and consequently κ_c increases with η. In a similar manner it is possible to calculate x_1 as

$$x_1 = -[F^{1\prime}(x_l,f,\kappa_l) + \partial F^l/\partial k\,\partial x\,\kappa_1]/F^{l\prime\prime}(x_l,f,\kappa_l) \tag{A31}$$

or, in general,

$$x_1 = -\kappa_l[F_2''(0)/F_1''(x_l)]\left[2\pi - \frac{(x_0+2\pi-x_l)^2-(x_l-x_0)^2}{2(\pi+x_0-x_l)}\right]. \tag{A32}$$

These results can be used to calculate the shifts in F'' and $\partial F/\partial\kappa$ required to calculate the effect of the nonlinearity on the period T. We find

$$\begin{aligned} F'' &= F^{l\prime\prime} + F^{1\prime\prime}\beta + \cdots, \\ \partial F/\partial\kappa &= \partial F^l/\partial\kappa + \partial F^1/\partial\kappa\beta + \cdots, \end{aligned} \tag{A33}$$

where

$$\begin{aligned} F^{1\prime\prime} &= -\kappa_l[F_2''(0)F_1'''(x_l)/F_1''(x_l)] \times\left[2\pi - \frac{[(x_0+2\pi-x_l)^2-(x_l-x_0)^2]}{2(\pi+x_0-x_l)}\right], \\ \frac{\partial F^1}{\partial\kappa} &= -2\kappa_l\left(\frac{F_2''(0)}{F_1''(x_l)}\right)\left[2\pi - \frac{[(x_0+2\pi-x_l)^2-(x_l-x_0)^2]}{2(\pi+x_0-x_l)} + \frac{F_2''(0)}{2}\right][(x_0+2\pi-x_l)^2-(x_l-x_0)^2]. \end{aligned} \tag{A34}$$

These results allow us to calculate the effect of a weak nonlinearity on the dynamics. As the nonlinearity parameter β is increased further, the period retains its $[\kappa-\kappa_c(\beta)]^{-1/2}$ dependence on κ. Thus writing $T(\beta)=A(\beta)[\kappa-\kappa_c(\beta)]^{-1/2}$ and $v(\beta)=B(\beta)[\kappa-\kappa_c(\beta)]^{1/2}$, we can see that a critical value of $\beta=\beta_c(\kappa)$ occurs given by the implicit equation

$$\kappa_c(\beta_c) = \kappa, \tag{A35}$$

where the period diverges and the average velocity tends to zero. For β close to β_c, we may use the Taylor-series expansion $\kappa_c(\beta)\approx\kappa-\kappa'(\beta_c-\beta)$; consequently,

$$\begin{aligned} T(\beta) &\approx T(\beta=\beta_c)[(\beta_c-\beta)/\beta_c]^{-1/2}, \\ v(\beta) &\approx v(\beta=\beta_c)[(\beta_c-\beta)/\beta_c]^{1/2}. \end{aligned} \tag{A36}$$

Equation (A36) is only valid as $\beta\to\beta_c$, but numerically this functional form appears to fit the data reasonably well all the way from $\beta=0$ to β_c.

APPENDIX B

To test the predictions of Eq. (24), we performed an analysis using just the first harmonic in the expansion of Eq. (23), expressing the position of the oscillator during the period $0<t<2\pi/\omega$ as

$$x(t) = A + \omega t + B\,\sin(\omega t+\beta), \tag{B1}$$

where ω is the characteristic overturning frequency of each single oscillator. During the rest of the period $2\pi/\omega<t<T$ (which forms a stick phase), $x=\sin^{-1}f$. Substituting Eq. (B1) into Eq. (4) and using the matching initial conditions [Eq. (12)] yields

$$\begin{aligned} -B\omega^2\sin(\omega t+\beta) + \gamma\omega + B\gamma\omega\,\cos(\omega t+\beta) \\ + \sin[A+\omega t+B\,\sin(\omega t+\beta)] \\ = f - 4\kappa B\,\sin^2\frac{\pi l\omega}{mNv}\,\sin(\omega t+\beta). \end{aligned} \tag{B2}$$

Equation (B2) is only valid to order $\sin(\omega t+\beta)$ and $\cos(\omega t+\beta)$, consistent with the ansatz Eq. (B1) [to find higher-order terms we would need to keep higher-order terms in Eq. (B1)]. We therefore expand $\sin[A+\omega t+B\ \sin(\omega t+\beta)]$ in Eq. (B2) in Bessel functions, using only the zeroth-, first-, and second-order Bessel functions to achieve harmonic balance

$$\begin{aligned}\sin[A+\omega t+B\ \sin(\omega t+\beta)] \simeq & -J_1(B)\sin(A-\beta)\\ &+[J_0(B)-J_2(B)]\cos(A-\beta)\\ &\times\sin(\omega t+\beta)\\ &+[J_0(B)+J_2(B)]\\ &\times\sin(A-\beta)\cos(\omega t+\beta)\\ &+\cdots . \end{aligned} \tag{B3}$$

Collecting terms showing the same time dependence results in three equations

$$-B\omega^2+[J_0(B)-J_2(B)]\cos(A-\beta)=-4\kappa B\ \sin^2\frac{\pi l\omega}{mNv}, \tag{B4a}$$

$$\gamma\omega-J_1(B)\sin(A-\beta)=f, \tag{B4b}$$

$$\gamma\omega B+[J_0(B)+J_2(B)]\sin(A-\beta)=0. \tag{B4c}$$

The matching of the quiescent and running solutions is done by using initial conditions [Eqs. (12)]

$$x(0)=x_0=\sin^{-1}f=A+B\ \sin\beta, \tag{B5a}$$

$$\dot{x}(0)=0=\omega+B\omega\ \cos\beta. \tag{B5b}$$

Equations (B4) and (B5) form a set of five equations for five variables: A, B, β, v, and ω. Substitution of Eq. (B4c) into Eq. (B4b) leads to

$$\omega=\frac{f/\gamma}{1+BJ_1(B)/[J_0(B)+J_2(B)]}. \tag{B6}$$

Since $J_0(x)=J_0(-x)$, $J_2(x)=J_2(-x)$, and $J_1(x)=-J_1(-x)$, there exist two trivially related solutions $B=\pm|B|$ for each value of ω. As $\omega\neq 0$, Eq. (B5b) implies that $B=-1/\cos\beta$ and thus $|B|>1$. For each value of $\cos\beta=\pm 1/|B|$, there exist two values of $\sin\beta=\pm\sqrt{|B^2|-1}/|B|$ for a total of four trivially related solutions depending on the quadrant in which β lies. In the following we shall assume that $0<\beta<\pi/2$ lies in the first quadrant and consequently $B=-|B|<-1$. Thus

$$\beta=\sin^{-1}[\sqrt{|B|^2-1}/|B|], \tag{B7a}$$

$$A=\sqrt{|B|^2-1}+x_0, \tag{B7b}$$

where Eqs. (B7) follow from Eq. (B5a). In principle, in addition to the four solutions discussed here, there exist two possibilities for $x_0=\sin^{-1}f$, one lying in the first quadrant and the other in the second. For the uncoupled oscillator only the first quadrant solution $\cos x_0>0$ is stable. We assume that this remains true for the coupled array in the presence of weak and intermediate coupling. Indeed, numerical simulations confirm this assumption. Thus we can write

$$\begin{aligned}\sin(A-\beta)=\frac{1}{|B|}\,[&(\sqrt{1-f^2}+f\sqrt{|B|^2-1})\sin\sqrt{|B|^2-1}\\ &+(f-\sqrt{1-f^2}\sqrt{|B|^2-1})\cos\sqrt{|B|^2-1}],\end{aligned} \tag{B8a}$$

$$\begin{aligned}\cos(A-\beta)=\frac{1}{|B|}\,[&(\sqrt{1-f^2}\sqrt{|B|^2-1}-f\ )\sin\sqrt{|B|^2-1}\\ &+(\sqrt{1-f^2}+f\sqrt{|B|^2-1})\cos\sqrt{|B|^2-1}].\end{aligned} \tag{B8b}$$

We solve Eqs. (B4) and (B5) in a sequential manner. First, eliminate the unknown angular frequency from Eqs. (B4b) and (B4c) and use Eq. (B7a) to derive an implicit equation for $|B(f)|$,

$$\begin{aligned}f=&[(\sqrt{1-f^2}+f\sqrt{|B|^2-1})\sin\sqrt{|B|^2-1}\\ &+(f-\sqrt{1-f^2}\sqrt{|B|^2-1})\cos\sqrt{|B|^2-1}]\\ &\times\left[\frac{J_1(|B|)}{|B|}+\frac{J_0(|B|)+J_2(|B|)}{|B|^2}\right].\end{aligned} \tag{B9}$$

Equation (B9) can be solved numerically to yield $|B(f)|$, a monotonically decreasing function of f for $f>f_c\approx 0.35$ with the finite limit $|B(f)|\to 1.523\ldots$ as $f\to 1.0$. At low values of the driving force multiple solutions of Eqs. (B8) appear (which may be unstable). Using $|B(f)|$, the variables $\beta(f)$ and $A(f)$ can also be found from Eqs. (B7). These variables describe the shape of the running solution and depend only on the driving force f.

The angular frequency $\omega(f,\gamma)$ is only a function of the force f and the damping coefficient γ; from Eq. (B6) and $|B(f)|$ we can write

$$\omega(f,\gamma)=\frac{\Omega(f)}{\gamma}, \tag{B10}$$

where

$$\Omega(f)=\frac{f}{1+|B|J_1(|B|)/[J_0(|B|)+J_2(|B|)]}=\frac{f}{1+B^2/2} \tag{B11}$$

is a monotonically increasing function of the driving force f. Having found an explicit expression for $\omega(f,\gamma)$, we are now in a position to use Eq. (B4a) to find the average velocity v from

$$\frac{\Omega^2(f)}{\gamma^2}+G(f)=4\kappa\ \sin^2\frac{\pi l\Omega(f)}{\gamma mNv}, \tag{B12}$$

where

$$\begin{aligned}G(f)=&\frac{1}{|B(f)|}\,\{J_0[|B(f)|]-J_2[|B(f)|]\}\\ &\times\cos[A(f)-\beta(f)].\end{aligned} \tag{B13}$$

We now can use expressions (B11) and (B13) to estimate the validity of the replacement $\sin(\pi l\Omega/\gamma mNv)\approx\pi l\Omega/\gamma mNv$. From Eq. (B11), $\Omega(f)$ has an upper bound of

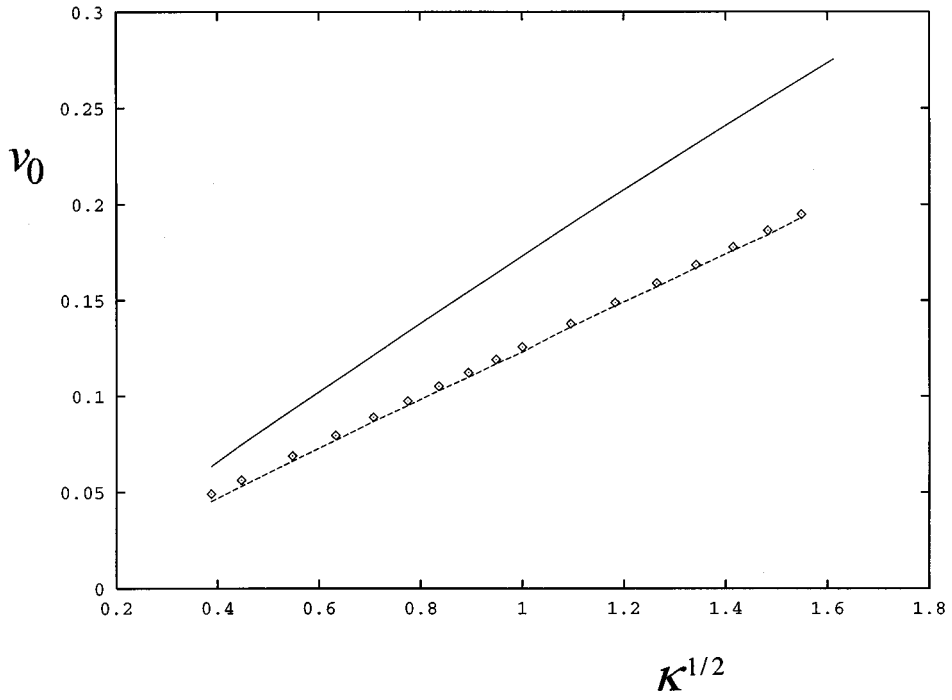

FIG. 9. Time-averaged minimal velocities of $N=25$ oscillators v_0 as a function of $\sqrt{\kappa}$ for the case of linear coupling. The upper curve denotes numerically calculated values of the average velocity, the bottom dotted line shows the theoretical curve [Eq. (B12)] and the points show the linearized expression $\sin x \approx x$ obtained from Eq. (B12). The other parameters are $f=0.9$ and $\gamma=0.7$. The initial conditions are $x_N(0)=5$, $\dot{x}_N(0)=0.8$, and $x_j(0)=\dot{x}_j(0)=0$ for all $j=1,\ldots,N-1$.

$1/[1+B(1)^2/2]=0.463$. From the Eq. (B13), $G(f)$ is bounded by $1/B(1)=0.66$ [in fact, our numerical calculations show that $G(f)<0.1$ for $0.5<f<1$]. Thus, for $\gamma=0.7$, $\mathcal{F}(f)$ is bounded by 1.1, so $\sqrt{\mathcal{F}/4\kappa} \leqslant \sqrt{1/4\kappa}$; therefore, for example, for $\kappa=1$, $\pi l\Omega/\gamma mNv \approx 0.5$. Thus our estimate is reasonable for $\kappa \geqslant 1$. We observe numerically that the linearization is a fair approximation for Eq. (B12) for a broader range of the coupling $\kappa>0.1$ (for the parameter values considered). We show in Fig. 9 the minimal values of the average velocity calculated numerically (upper curve) compared with the average velocity derived from Eq. (B12) (dotted line); the points show the linearized version of Eq. (B12). Both curves fit the $\sqrt{\kappa}$ dependence on the coupling constant well; the predicted values of the average velocity v for a given parameter range are about 20% lower than the actual numerical values.

[1] F. P. Bowden and D. T. Tabor, *Friction and Lubrication of Solids* (Clarendon, Oxford, 1986); E. Rabinowics, *Friction and Wear of Materials* (Wiley, New York, 1965).

[2] J. N. Israelachvili, Surf. Sci. Rep. **14**, 109 (1992); B. N. Persson, Phys. Rev. B **48**, 18 140 (1993); J. Chem. Phys. **103**, 3849 (1995); B. Brushan, J. N. Israelachvili, and U. Landman, Nature **374**, 13 (1995); J. Krim, Comments Condens. Matter Phys. **17**, 263 (1995).

[3] R. Burridge and L. Knopoff, Bull. Seismol. Soc. Am. **57**, 341 (1967); J. M. Carlson and J. S. Langer, Phys. Rev. A **40**, 6470 (1989); J. S. Langer and C. Tang, Phys. Rev. Lett. **67**, 1043 (1991); J. M. Carlson, J. S. Langer, B. E. Shaw, and C. Tang, Phys. Rev. A **44**, 884 (1991); L. Knopoff, J. A. Landoni, and M. S. Abinante, *ibid*. **46**, 7445 (1992); J. S. Langer, *ibid*. **46**, 3123 (1992); K. Runde, Phys. Rev. E **49**, 2597 (1994); F.-J. Elmer, *ibid*. **50**, 4470 (1994); M. Weiss and F.-J. Elmer, Phys. Rev. B **53**, 7539 (1996).

[4] H. Yoshizawa, P. McGuiggan, and J. Israelachvili, Science **259**, 5099 (1993); D. P. Vallette and J. P. Gollub, Phys. Rev. E **47**, 820 (1993); B. Lin and P. L. Taylor, *ibid*. **49**, 3940 (1994); T. Baumberger, F. Heslot, and B. Perrin, Nature **367**, 544 (1994); F. Heslot, T. Baumberger, B. Perrin, B. Caroli, and C. Caroli, Phys. Rev. E **49**, 4973 (1994); T. Baumberger, C. Caroli, B. Perrin, and O. Ronsin, *ibid.* **51**, 4005 (1995); D. Pisarenko and P. Mora, Pure Appl. Geophys. **142**, 447 (1994); D. C. Hong and S. Yue, Phys. Rev. Lett. **74**, 254 (1995), M. G. Rozman, M. Urbakh, and J. Klafter, Phys. Rev. Lett. **77**, 683 (1996); Phys. Rev. E **54**, 6485 (1996).

[5] A. Ruina, J. Geophys. Res. **88**, 10 359 (1983); J. R. Rice and A. L. Ruina, J. Appl. Mech. **50**, 343 (1983); Chao Gao, D. Kuhlmann-Wilsdorf, and D. D. Makel, Wear **173**, 1 (1994).

[6] H. J. Feder and J. Feder, Phys. Rev. Lett. **66**, 2669 (1991); Z. Olami and K. Christensen, Phys. Rev. A **46**, R1720 (1992); G. L. Vasconcelos, G. L. de Sousa Vieira, and S. R. Nagel, Physica A **191**, 69 (1992); A. Johansen, P. Dimon, C. Ellegaard, J. S. Larsen, and H. H. Rugh, Phys. Rev. E **48**, 4779 (1993); E. J. Ding and Y. N. Lu, Phys. Rev. Lett. **70**, 3627 (1993); Y. N. Lu and E. J. Ding, Phys. Rev. E **48**, R21 (1993); M. de Sousa and H. J. Hermann, *ibid*. **49**, 4534 (1994); P. Espanol, *ibid*. **50**, 227 (1994).

[7] J. Krim, E. T. Watts, and J. Digel, J. Vac. Sci. Technol. A **8**, 3417 (1990); J. Krim, D. H. Solina, and R. Chiarello, Phys. Rev. Lett. **66**, 181 (1991); S. Granick, Science **253**, 1374 (1991); G. Reiter, A. L. Demirel, and S. Granick, *ibid*. **263**, 1741 (1994); T. Strunz and F. J. Elmer, in *Physics of Sliding Friction*, edited by B. N. J. Persson and E. Tossati (Kluwer, Dordrecht, 1996); M. Granato, R. S. Baldan, and S. C. Ying, C. Daly, and J. Krim, Phys. Rev. Lett. **76**, 803 (1996).

[8] D. Tabor, in *Microscopic Aspects of Adhesion and Lubrication, Tribology Series 7*, edited by J. M. Georges (Elsevier, New York, 1982), pp. 651–682; U. Landman, W. D. Luedtke, N. A. Burnham, and R. J. Colton, Science **248**, 454 (1990); P. A. Thompson and M. O. Robbins, Phys. Rev. A **41**, 6830 (1990); Science **250**, 4982 (1990); W. Zhong and D. Tomanek, Phys. Rev. Lett. **64**, 3054 (1990); J. B. Sokoloff, *ibid*. **66**, 965 (1991); U. Landman and W. D. Luedtke, J. Vac. Sci. Technol. B **9**, 414 (1991); R. M. Overney, H. Takano, M. Fujihira, W. Paulus, and H. Ringsdorf, Phys. Rev. Lett. **72**, 3546 (1994).

[9] The Frenkel-Kontorova model was introduced in Y. I. Frenkel and T. Kontorova, Zh. Eksp. Theor. Fiz. **8**, 1340 (1938). The static properties of the FK model for infinite chains were intensively studied by Aubry and co-workers [S. Aubry, J. Phys. C **16**, 1593 (1983), and references therein]. The static properties of the finite FK chains can be found in Y. Braiman, J. Baumgarten, and J. Klafter, Phys. Rev. B **47**, 11 159 (1993). The dynamics of the finite FK model can be found in S. Stoyanov and H. Müller-Krumbhaar, Surf. Sci. **159**, 49 (1985); K. Shinjo and M. Hirano, *ibid*. **283**, 473 (1993).

[10] Y. Braiman, I. Goldhirsch, and J. Klafter, Phys. Rev. E **50**, 838 (1994), and references therein.

[11] For high values of $\gamma>1$ (the overdamped situation), behavior other than linear wave solutions [Eq. (6)] are more likely to occur, thus $\gamma>1$ does not unconditionally imply usage of Eq. (11) resulting in $v\approx(\kappa-\kappa_c)^{1/2}$.

[12] We performed numerical simulation for an underdamped case where the contribution of the inertia term is important. Specifically, we used the value of the linear friction coefficient $\gamma=0.2$. Indeed, for the underdamped situation the ansatz [Eq. (11)] is not correct and the result [Eq. (13)] is not valid. We found that the average velocity v depends on κ as $v\approx\sqrt{(v_0^2+c\kappa)}$, with v_0^2 and c constants.

[13] We plan to present the details: Y. Braiman, F. Family, and H. G. E. Hentschel (unpublished).

[14] Y. Braiman, F. Family, and H. G. E. Hentschel, Phys. Rev. E **53**, R3005 (1996).

[15] It has been found [see M. Büttiker and H. Thomas, Phys. Rev. A **37**, 235 (1988)] that for the continuum limit and describing the propagating kink solution, $v=\sqrt{\kappa}/\gamma\phi_g(f)[1+\chi^2\phi_g(f)]^{-1/2}$, with $\chi=$const. In principle, there are two possible ways our solution (Appendix B) can be continued towards the continuum limit: (a) increasing the coupling constant κ while keeping all the other parameters unchanged and (b) increasing γ and the forcing f (for $\gamma>1$, f must be higher than 1 to obtain running solutions). Possibility (a), which would be consistent with Appendix B, is observed to lead to the breaking of symmetry, thus the solution [Eq. (6)] will not be valid. Possibility (b) would indeed lead to the solution [Eq. (6)]; however, because $f>1$ and there are no fixed points for an uncoupled oscillator, the initial conditions [Eqs. (B5)] would not be correct, thus leading to expressions different from those derived in the Appendix B.